

OPEN ACCESS

Estimation of thermo-physical and transport properties with Bayesian inference using transient liquid crystal thermography experiments

To cite this article: B Konda Reddy *et al* 2012 *J. Phys.: Conf. Ser.* **395** 012082

View the [article online](#) for updates and enhancements.

Related content

- [Experimental Study of Endwall Heat Transfer in a Linear Cascade](#)
Lei Wang, Bengt Sundén, Valery Chernoray *et al.*
- [Thermal management of electronics using phase change material based pin fin heat sinks](#)
R Baby and C Balaji
- [A novel approach to thermochromic liquid crystal calibration using neural networks](#)
G S Grewal, M Bharara, J E Cobb *et al.*

Recent citations

- [Evaluation of artificial neural network in data reduction for a natural convection conjugate heat transfer problem in an inverse approach: experiments combined with CFD solutions](#)
M K Harsha Kumar *et al*
- [Coupled POD-Bayesian estimation of the parameters of mathematical model of the packed-bed drying of cherry stones](#)
Zbigniew Buliski *et al*
- [A Markov Chain Monte Carlo-Metropolis Hastings Approach for the Simultaneous Estimation of Heat Generation and Heat Transfer Coefficient from a Teflon Cylinder](#)
Harsha Kumar *et al*



ECS **240th ECS Meeting**
Oct 10-14, 2021, Orlando, Florida

Register early and save up to 20% on registration costs

Early registration deadline Sep 13

REGISTER NOW

Estimation of thermo-physical and transport properties with Bayesian inference using transient liquid crystal thermography experiments

B Konda Reddy¹, N Gnanasekaran² and C Balaji³

^{1,2} Research Scholar, Heat Transfer and Thermal Power Laboratory, Department of Mechanical Engineering, Indian Institute of Technology Madras, Chennai- 600 036, Tamilnadu, India.

³ Professor, Heat Transfer and Thermal Power Laboratory, Department of Mechanical Engineering, Indian Institute of Technology Madras, Chennai- 600 036, Tamilnadu, India.

E-mail: balaji@iitm.ac.in

Abstract. An inverse methodology is proposed to estimate thermo-physical and transport properties individually and simultaneously from in-house experimental data obtained using the transient Liquid Crystal Thermography (LCT) technique. A vertical rectangular fin made of mild steel and size of $75 \times 250 \times 3$ ($L \times W \times t$) (all in mm) has been used. Thermochromic Liquid Crystals (TLCs) are used to obtain transient temperature distribution along the fin surface to determine the temperature dependent heat transfer coefficient, h_θ and the thermal diffusivity, α of the fin. The variation of heat transfer coefficient is considered as a power law function of temperature excess ($h_\theta = a''\theta_{(x,t)}^b$) and is derived from the basic Nusselt number equation, $Nu_\theta = aRa_\theta^b$ used for laminar natural convection for a vertical plate in ambient air. Using this functional form, the 1-D transient fin equation solved using the finite difference technique for assumed values of 'a' and ' α '. Treating the inverse problem as a one parameter estimation in 'a' or ' α ' or a two parameter estimation problem in 'a' and ' α ', the sum of the squares of the difference between the TLC measured and simulated temperatures are minimized with the Bayesian frame work in the inverse model to determine the point estimates for 'a' and ' α '. Two point estimates namely the (i) mean and (ii) maximum a posteriori (MAP) are used to report the retrieved quantities together with the associated standard deviation.

1. Introduction

Parameter estimation in inverse heat transfer concerns the estimation of causes (thermo-physical and transport properties) from the effects. This is invariably done by using an optimization technique. Figure 1 shows the general procedure to estimate parameters in inverse heat transfer problems. In the present work, Bayesian inference has been used for solving the inverse problem. The advantage of the Bayesian inference is, that it allows for incorporation of (i) noise in the data and (ii) prior information in the estimation of parameters. A detailed account of inverse heat conduction and ill posed problems is given by Beck et al. [1]. Hueang and Yan [2] estimated the temperature dependent thermal conductivity and heat capacity simultaneously using a transient data for an inverse problem.

While solving the transient fin temperature equation to determine the temperature distribution in a forward model, invariably the average heat transfer coefficient has been considered in literature. However, this quantity, in natural convection, varies with the

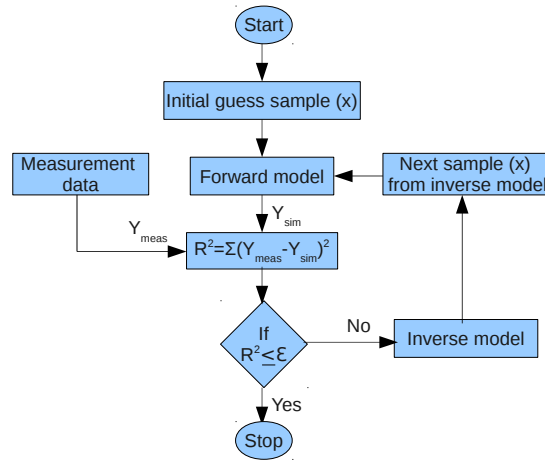


Figure 1. General procedure for a parameter estimation in an inverse heat transfer problem.

temperature excess along the length of the fin. The heat transfer coefficient varies with temperature excess in a power law form. Unal [3] and Laor and Kalman [4] considered the power law formula in their analytical and numerical analysis for fin problems. Orzechowski [5] considered the power law form in his experimental analysis of the fin problem. The temperature dependent heat transfer coefficient can be derived from the basic Nusselt number equation used for laminar natural convection as follows.

$$Nu_{\theta} = aRa_{\theta}^b = a \left(\frac{g\beta\theta_{(x,t)}L^3}{\nu\alpha_f} \right)^b = a'\theta_{(x,t)}^b \quad (1)$$

$$h_{\theta} = \frac{Nu_{\theta}k_f}{L} = \frac{a \left(\frac{g\beta\theta_{(x,t)}L^3}{\nu\alpha_f} \right)^b k_f}{L} = a''\theta_{(x,t)}^b \quad (2)$$

The goal is to retrieve ‘a’ in equation (1) from Liquid Crystal Thermography (LCT) experiments and inverse heat transfer, with a view to estimating the temperature dependent heat transfer coefficient ‘ h_{θ} ’ in equation (2) by considering exponent ‘b’ as 0.25 (for laminar natural convection). The temperature field required for the estimation can be obtained with the Liquid Crystal Thermography (LCT) technique. LCT is an inexpensive thermal imaging technique for mapping surface temperature distribution. Thermochromic Liquid Crystals (TLCs) are Chiral (twisted) molecular structures and show colors by selectively reflecting incident white light. A comprehensive study of TLCs is given in Hallcrest [6]. Abdullah et al. [7] give an account of the basic issues associated with TLC calibration widely in the field of heat transfer.

The present work discusses the estimation of temperature dependent heat transfer coefficient, ‘ h_{θ} ’ and thermal diffusivity, ‘ α ’ for a vertical rectangular fin by combining temperature measurements from unsteady heat transfer experiments using LCT and the Bayesian inference.

2. Experimental set up

The schematic and a photographic view of the experimental setup are shown in figures 2 and 3 respectively. A vertical fin made of mild steel in rectangular cross-section, $75 \times 250 \times 3$ ($L \times W \times t$) (all in mm) is placed on two heated horizontal aluminium blocks that acts as a horizontal base. A heater is placed below the aluminium blocks and it is insulated with glass wool to restrict the heat flow from the bottom side of the heater plate. K-type thermocouples are inserted along the length of the fin and R40C5W TLC sheet is pasted on the surface of the fin. The color

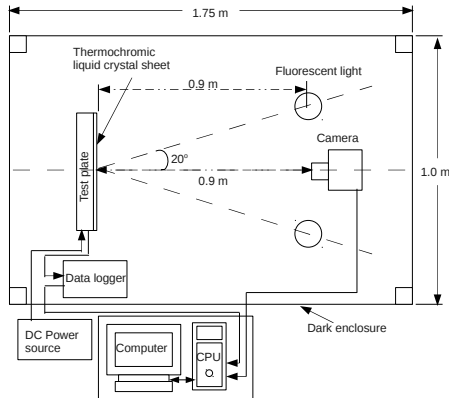


Figure 2. Schematic diagram of the experimental set up.

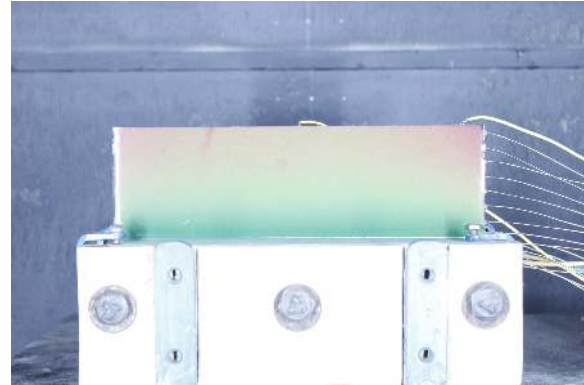


Figure 3. Photographic view of the experimental set up.

change of the TLC sheet as a consequence of the temperature distribution in the fin is captured with a Canon 500D digital camera. Anderson and Baughn [8] examined the spectral effects of a variety of illumination sources. In the present, the illumination light source is provided with two Philips 20 W, 6500 K cool day fluorescent lights. The camera and illumination sources are kept at a distance of 0.9 m away from the test setup. The illumination source is arranged off-axis by 20° and the camera is placed on the axis. Chan et al. [9] investigated the effect of variation in illumination viewing angles on the LCT results and concluded set of $0-20^\circ$ is recommended for best results. The test setup, camera and illumination sources are provided in a dark enclosure of dimensions $1.75 \times 1 \times 1.2$ (all in m), to isolate the measurements from ambient disturbances and secondary illumination sources.

3. Liquid crystal thermography

3.1. Digital image processing

From Gonzalez et al. [10], the hue (H), saturation (S) and intensity (I) are calculated from the RGB color space to HSI color space, color image processing has been done for converting colors from RGB to HSI in MATLAB.

$$\begin{cases} H = \begin{cases} \theta, & \text{if } B \leq G \\ 360 - \theta, & \text{if } B > G \end{cases} \text{ with } \theta = \cos^{-1} \left(\frac{0.5[(R-G)+(R-B)]}{[(R-G)^2+(R-B)(G-B)]^{\frac{1}{2}}} \right) \\ S = 1 - \frac{3}{(R+G+B)}[\min(R, G, B)] \\ I = \frac{1}{3}(R + G + B) \end{cases} \quad (3)$$

3.2. Calibration of liquid crystal sheet

In situ calibration of TLC sheet with thermocouples has been done by plotting thermocouple temperatures against normalized hue values, as shown in figure 4. The uncertainty of the TLC sheet is $\pm 0.17^\circ\text{C}$. The trend of the temperature versus hue has been applied to each pixel location on the surface of the fin to obtain the local surface temperatures, as shown in figure 5.

4. Forward model

From the experimental data (figure 5), it is seen that the temperature distribution over the fin surface is indeed one dimensional. Let $\theta_{(x,t)} = (T_{(x,t)} - T_\infty)$, then the partial differential equation for the control volume element on a transient fin is,

$$\frac{\partial^2 \theta_{(x,t)}}{\partial x^2} - \frac{h_{\theta p}}{k_s t W} \theta_{(x,t)} = \frac{\rho c_p}{k_s} \frac{\partial \theta_{(x,t)}}{\partial t} \quad (4)$$

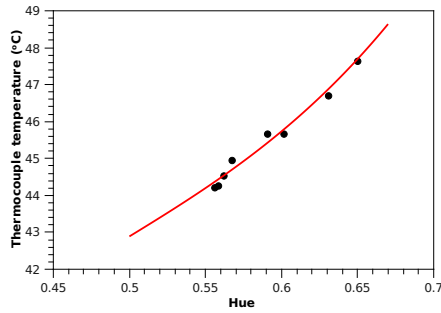


Figure 4. Calibration curve of the TLC sheet relating temperature with hue.

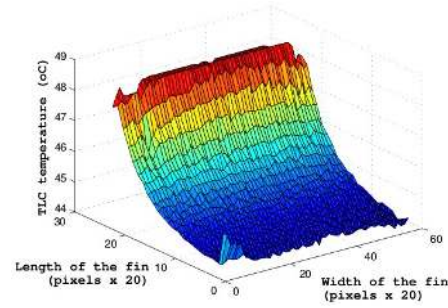


Figure 5. Temperature field on the surface of the fin by applying the calibration procedure.

Substitute for h_θ in equation (4), we have

$$\frac{\partial^2 \theta_{(x,t)}}{\partial x^2} - \frac{a \left(\frac{g\beta\theta_{(x,t)}L^3}{\nu\alpha_f} \right)^b k_f p}{k_s L t W} \theta_{(x,t)} = \frac{1}{\alpha} \frac{\partial \theta_{(x,t)}}{\partial t} \quad (5)$$

The initial and boundary conditions for solving equation (5) are, at $t=0$ s, $\theta_{(x,0)} = f(x)$; at $x=0$ m, $\theta_{(0,t)} = f_1(t)$ and at $x=L$ m, $\theta_{(L,t)} = f_2(t)$.

The functions f , f_1 and f_2 are obtained directly from measurements by using regression. Equation (5), is in a form to retrieve ‘ a ’ and ‘ α ’, once $\theta_{(x,t)}$ is available from experiments. In the forward model, for assumed values of parameters ‘ a ’ and ‘ α ’ individually and simultaneously, equation (5) can be solved numerically using finite difference method with an explicit scheme to march in time and the temperature distribution along the length of the fin for various time instances can be computed. A grid independence study showed that 16 equi-spaced nodes are sufficient.

5. Inverse model

The temperature distribution along the length of the fin, $\theta_{(x,t)}$ is measured with LCT technique at different instants of time. For this study, experiments were done for a power level of 19.98 W. Upon reaching steady state the power was switched and the temperature time history is logged. Bayesian inference is then used to match the experimentally obtained temperature distribution with the distribution obtained by solving equation (5) for guess values of ‘ a ’ and ‘ α ’. Treating equation (5) as a single (‘ a ’ or ‘ α ’) or two (‘ a ’ and ‘ α ’) parameter estimation, the sum of the squares of the difference between the measured and simulated temperatures is first calculated as follows.

$$R^2 = \sum_{j=1}^M \sum_{i=1}^N \left(\theta_{i,meas}^j - \theta_{i,sim}^j \right)^2 \quad (6)$$

Where ‘ i ’ stands for spatial location node and ‘ j ’ stands for time under consideration. In this study $N=16$ and $M=13$. The Bayes theorem relates the experimental data Y and the state vector x as

$$P(x/Y) = \frac{P(Y/x)P(x)}{P(Y)} = \frac{P(Y/x)P(x)}{\int P(Y/x)P(x)dx} \quad (7)$$

Where $P(x/Y)$ is called the posterior probability density function (PPDF), $P(Y/x)$ is the likelihood density function, $P(x)$ is the prior density function and $P(Y)$ is the normalizing

constant. The likelihood density function for the measured data points is as follows,

$$P(Y/x) = \frac{1}{(\sqrt{2\pi\sigma^2})^n} e^{-\left(\frac{(Y-F(x))^T(Y-F(x))}{2\sigma^2}\right)} = \frac{1}{(\sqrt{2\pi\sigma^2})^n} e^{-\left(\frac{\chi^2}{2}\right)} \quad (8)$$

where $n=N \times M$, $\chi^2 = \frac{R^2}{\sigma^2}$, Y is the measurement data vector of dimension n and $F(x)$ is the solution to the forward model with the parameter vector x . The prior density function $P(x)$ typically follows a uniform or normal distribution. In the case of a uniform prior, $P(x)$ is the same for all values of x . In this study, whenever a prior is given, $P(x)$ will be assumed to a normal distribution with a mean of μ_p and a standard deviation of σ_p . For a normal prior, $P(x)$ is given by

$$P(x) = \frac{1}{\sqrt{2\pi\sigma_p^2}} e^{-\frac{(x-\mu_p)^2}{2\sigma_p^2}} \quad (9)$$

5.1. Single parameter estimation

From equation (8) and (9), the PPDF for single parameter (for estimating either 'a' or ' α ') becomes

$$P(x/Y) = \frac{\frac{1}{(\sqrt{2\pi\sigma^2})^n} e^{-\left(\frac{\chi^2}{2}\right)} \times \frac{1}{\sqrt{2\pi\sigma_p^2}} e^{-\frac{(x-\mu_p)^2}{2\sigma_p^2}}}{\int \left[\frac{1}{(\sqrt{2\pi\sigma^2})^n} e^{-\left(\frac{\chi^2}{2}\right)} \times \frac{1}{\sqrt{2\pi\sigma_p^2}} e^{-\frac{(x-\mu_p)^2}{2\sigma_p^2}} \right] dx} = \frac{e^{-\left[\frac{\chi^2}{2} + \frac{(x-\mu_p)^2}{2\sigma_p^2}\right]}}{\int e^{-\left[\frac{\chi^2}{2} + \frac{(x-\mu_p)^2}{2\sigma_p^2}\right]} dx} \quad (10)$$

The mean and the variance estimate of x are as follows for discrete data values of x ,

$$\bar{x} = \frac{\sum_i x_i \times e^{-\left[\frac{\chi^2}{2} + \frac{(x_i-\mu_p)^2}{2\sigma_p^2}\right]}}{\sum_i e^{-\left[\frac{\chi^2}{2} + \frac{(x_i-\mu_p)^2}{2\sigma_p^2}\right]}} \quad \text{and} \quad \sigma_x^2 = \frac{\sum_i (x_i - \bar{x})^2 \times e^{-\left[\frac{\chi^2}{2} + \frac{(x_i-\mu_p)^2}{2\sigma_p^2}\right]}}{\sum_i e^{-\left[\frac{\chi^2}{2} + \frac{(x_i-\mu_p)^2}{2\sigma_p^2}\right]}} \quad (11)$$

5.2. Two parameter estimation

For two parameter estimation, the probability distribution is two dimensional for a given values of x and y . From Bayes theorem, the PPDF becomes

$$P(x, y/Y) = \frac{P(Y/x, y)P(x)P(y)}{\iint P(Y/x, y)P(x)P(y)dx dy} = \frac{e^{-\left[\frac{\chi^2}{2} + \frac{(x-\mu_{x,p})^2}{2\sigma_{x,p}^2} + \frac{(y-\mu_{y,p})^2}{2\sigma_{y,p}^2}\right]}}{\iint e^{-\left[\frac{\chi^2}{2} + \frac{(x-\mu_{x,p})^2}{2\sigma_{x,p}^2} + \frac{(y-\mu_{y,p})^2}{2\sigma_{y,p}^2}\right]} dx dy} \quad (12)$$

Marginal distribution have been used to define the PPDF for x and y .

$$P(x/Y) = \frac{P(Y/x, y)P(x)P(y)}{\int P(Y/x, y)P(x)P(y)dy} \quad \text{and} \quad P(y/Y) = \frac{P(Y/x, y)P(x)P(y)}{\int P(Y/x, y)P(x)P(y)dx} \quad (13)$$

The mean and the variance estimates for x can be obtained by adding the row probability sum and the mean and the variance estimates for y can be obtained by adding the column probability sum. The mean and the variance estimate of x are as follows for discrete data values (x, y),

$$\bar{x} = \frac{\sum_i x_i \times e^{-\left[\frac{\chi^2}{2} + \frac{(x_i-\mu_{x,p})^2}{2\sigma_{x,p}^2} + \frac{(y_i-\mu_{y,p})^2}{2\sigma_{y,p}^2}\right]}}{\sum_i e^{-\left[\frac{\chi^2}{2} + \frac{(x_i-\mu_{x,p})^2}{2\sigma_{x,p}^2} + \frac{(y_i-\mu_{y,p})^2}{2\sigma_{y,p}^2}\right]}} \quad \text{and} \quad \sigma_x^2 = \frac{\sum_i (x_i - \bar{x})^2 \times e^{-\left[\frac{\chi^2}{2} + \frac{(x_i-\mu_{x,p})^2}{2\sigma_{x,p}^2} + \frac{(y_i-\mu_{y,p})^2}{2\sigma_{y,p}^2}\right]}}{\sum_i e^{-\left[\frac{\chi^2}{2} + \frac{(x_i-\mu_{x,p})^2}{2\sigma_{x,p}^2} + \frac{(y_i-\mu_{y,p})^2}{2\sigma_{y,p}^2}\right]}} \quad (14)$$

Similarly, the mean and the variance estimate of y is as follows for a given two parameter discrete data values (x, y) ,

$$\bar{y} = \frac{\sum_i y_i \times e^{-\left[\frac{\chi^2}{2} + \frac{(x_i - \mu_{x,p})^2}{2\sigma_{x,p}^2} + \frac{(y_i - \mu_{y,p})^2}{2\sigma_{y,p}^2}\right]}}{\sum_i e^{-\left[\frac{\chi^2}{2} + \frac{(x_i - \mu_{x,p})^2}{2\sigma_{x,p}^2} + \frac{(y_i - \mu_{y,p})^2}{2\sigma_{y,p}^2}\right]}} \text{ and } \sigma_y^2 = \frac{\sum_i (y_i - \bar{y})^2 \times e^{-\left[\frac{\chi^2}{2} + \frac{(x_i - \mu_{x,p})^2}{2\sigma_{x,p}^2} + \frac{(y_i - \mu_{y,p})^2}{2\sigma_{y,p}^2}\right]}}{\sum_i e^{-\left[\frac{\chi^2}{2} + \frac{(x_i - \mu_{x,p})^2}{2\sigma_{x,p}^2} + \frac{(y_i - \mu_{y,p})^2}{2\sigma_{y,p}^2}\right]}} \quad (15)$$

In the preceding discussion $x = a$ and $y = \alpha$.

6. Results and Discussion

Experiments are done according to the color-temperature response of the TLC sheet. In the transient cooling phase for the first 120 s, the color-temperature response is considered for the retrieval of parameters. In the two minutes span, for every 10 seconds the temperature data has been captured. Results have been obtained for two cases (i) by considering data at 13 time instances and (ii) 3 time instances (30, 60 and 90 s from the switching off the power). Prior information has been obtained based on results for a case without prior and these are shown in table 1. The thermal conductivity of the mild steel fin is assumed as 50 W/m-K. The range of 'a' is 0.1 to 2 and the range of ' α ' is 1×10^{-7} - 1×10^{-4} . The optimum number of samples required for the analysis is considered as 200, as shown in table 2. For the two parameter estimation a total of $200 \times 200 = 40000$ samples were used.

Table 1. Parameters of the Gaussian prior for 'a' and ' α ' used in the retrieval.

Sl.No.	Parameter	Mean	SD
1	a	$\mu_{a,p}=0.7$	$\sigma_{a,p}=0.01$
2	α	$\mu_{\alpha,p}=1.5 \times 10^{-5}$	$\sigma_{\alpha,p}=0.65 \times 10^{-7}$

Table 2. Number of samples required for the retrieval of 'a' and ' α '.

Sl.No.	No. of samples	'a'			' α ', m ² /s		
		Mean	MAP	SD	Mean	MAP	SD
1	50	0.7579	0.7592	0.0264	1.8040×10^{-5}	1.8449×10^{-5}	1.4535×10^{-6}
2	200	0.7579	0.7588	0.0265	1.8043×10^{-5}	1.7670×10^{-5}	1.4468×10^{-6}
3	500	0.7579	0.7587	0.0265	1.8043×10^{-5}	1.7718×10^{-5}	1.4468×10^{-6}

6.1. Estimation of 'a' and ' α ' individually

From the TLC temperature distribution data, the parameters 'a' and ' α ' are first retrieved individually with mean, MAP and standard deviation for (i) with prior and (ii) without prior for 3 and 13 time instances respectively, as shown in table 3. The PPDFs for 'a' and ' α ' for the corresponding range are shown in figures 6 and 7 respectively. It can be seen that with the injection of prior, the SD of the estimates come down significantly.

Table 3. Results for the estimation of 'a' and ' α ' individually.

Sl.No.	No. of time instances		'a'			' α ', m ² /s		
			prior	Mean	MAP	SD	Mean	MAP
1	3	w/o prior	0.7579	0.7588	0.0265	1.8043×10^{-5}	1.7670×10^{-5}	1.4468×10^{-6}
		with prior	0.7073	0.7111	0.0093	1.5160×10^{-5}	1.5160×10^{-5}	1.3511×10^{-9}
2	13	w/o prior	0.7282	0.7302	0.0133	1.6125×10^{-5}	1.6164×10^{-5}	6.0460×10^{-7}
		with prior	0.7102	0.7111	0.0080	1.5160×10^{-5}	1.5160×10^{-5}	8.8023×10^{-10}

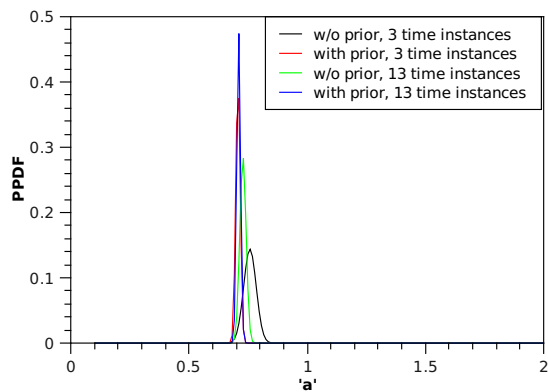


Figure 6. PPDF of ‘a’ for single parameter estimation.

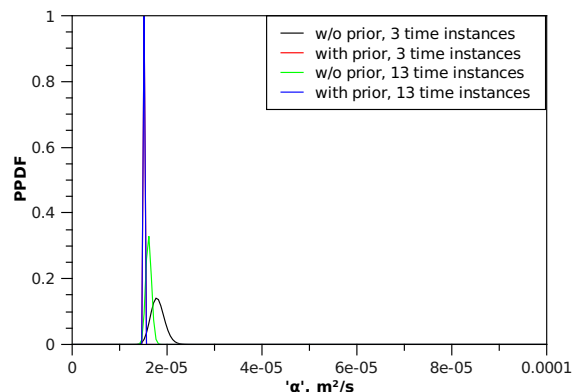


Figure 7. PPDF of ‘ α ’ for single parameter estimation.

6.2. Simultaneous estimation of ‘a’ and ‘ α ’

From the TLC temperature distribution data, the parameters ‘a’ and ‘ α ’ were retrieved simultaneously with mean, MAP and standard deviation for (i) with prior and (ii) without prior at 3 and 13 time instances, as shown in table 4. The PPDFs for ‘a’ and ‘ α ’ for the corresponding range are shown in figures 8 and 9 respectively. The dramatic reduction in SD with the injection of priors is seen for both ‘a’ and ‘ α ’.

Table 4. Results of the simultaneous estimation of ‘a’ and ‘ α ’.

Sl.No.	No. of time instances	prior	‘a’			‘ α , m ² /s		
			Mean	MAP	SD	Mean	MAP	SD
1	3	w/o prior	0.6552	0.6538	0.1089	2.6159×10^{-5}	1.6666×10^{-5}	1.6110×10^{-5}
		with prior	0.7068	0.7111	0.0093	1.5160×10^{-5}	1.5160×10^{-5}	1.4345×10^{-9}
2	13	w/o prior	0.7496	0.7397	0.0506	1.4395×10^{-5}	1.3654×10^{-5}	1.8805×10^{-6}
		with prior	0.7089	0.7111	0.0080	1.5160×10^{-5}	1.5160×10^{-5}	1.2686×10^{-9}

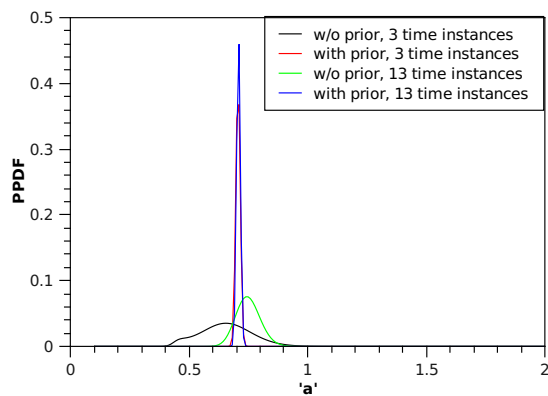


Figure 8. PPDF of ‘a’ for two parameter estimation.

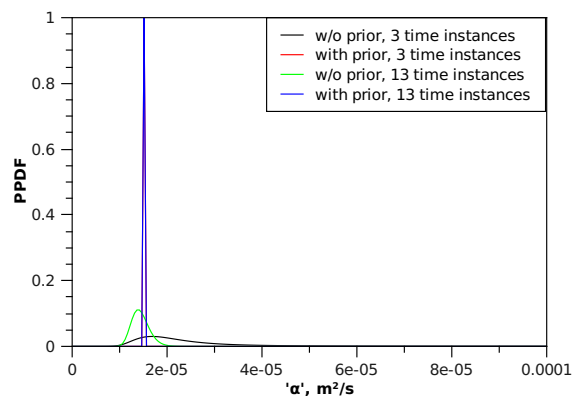


Figure 9. PPDF of ‘ α ’ for two parameter estimation.

Once the parameters ‘a’ and ‘ α ’ are retrieved, the parameter ‘a’ has been used to calculate temperature dependent heat transfer coefficient, ‘ h_θ ’. The variation of ‘ h_θ ’ with x at three time instances is shown in figure 10. It can be seen that with increasing time, ‘ h_θ ’ goes down at all x, as expected. Using the retrieved ‘ h_θ ’ and ‘ α ’, the forward model was re-run and simulated temperatures thus obtained were compared with TLC measurements. The results of the comparison shown in figure 11 establish the soundness of the retrievals.

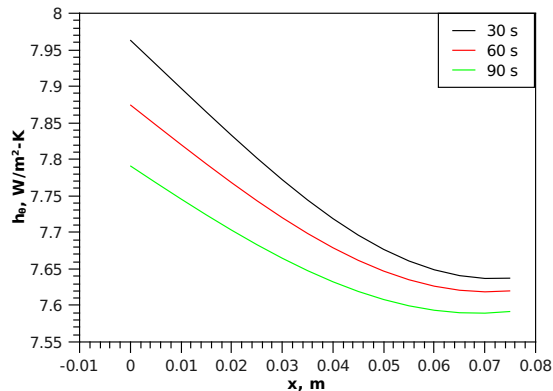


Figure 10. Temperature dependent heat transfer coefficient along the length of the fin for the retrieved value of ‘a’.

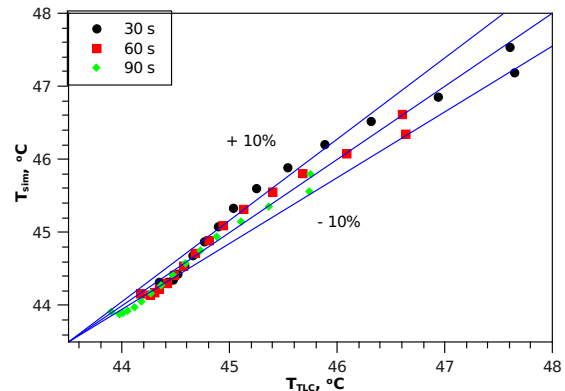


Figure 11. Parity plot between simulated and TLC measured temperatures for the retrieved value of ‘a’ and ‘ α ’.

7. Conclusions

Transient, natural convection experiments were conducted on a vertical rectangular fin. Thermochromic Liquid Crystals (TLCs) were used for obtaining the temperature distribution over the surface of the fin. The experimental results are married with a forward model to retrieve parameters ‘a’ (and thus the temperature dependent heat transfer coefficient, ‘ h_θ ’) and ‘ α ’ by minimizing the R^2 in inverse model using Bayesian inference. Reliable and repeatable values of ‘a’ and ‘ α ’ were obtained with a good accuracy. Priors were found to significantly improve retrieval accuracies. The present study thus offers a reasonably inexpensive method to estimate temperature dependent heat transfer coefficient and thermal diffusivity simultaneously with TLC measurements.

8. References

- [1] Beck J V, Blackwell B and Clair C S 1985 *Inverse Heat Conduction-Ill Posed Problems* (New York: Wiley)
- [2] Hueang C and Yan J 1995 *International Journal of Heat and Mass Transfer* **38** 3433–3441
- [3] Unal H 1985 *International Journal of Heat and Mass Transfer* **28** 2279–2284
- [4] Laor K and Kalman H 1996 *International Journal of Heat and Mass Transfer* **39** 19932003
- [5] Orzechowski T 2007 *Experimental Thermal and Fluid Science* **31** 947955
- [6] LCRHallcrest 1991 *Handbook of Thermochromic Liquid Crystal Technology* (<http://www.hallcrest.com/randt.cfm> (accessed on 10.02.2011))
- [7] Abdullah N, Talib A R A, Jaafar A A, Salleh M A M and Chong W T 2010 *Experimental Thermal and Fluid Science* **34** 1089–1121
- [8] Anderson M R and Baughn J W 2005 *ASME Journal of Heat Transfer* **127** 581–587
- [9] Chan T L, Ashforth-Frost S and Jambunathan K 2001 *International Journal of Heat and Mass Transfer* **44** 2209–2223
- [10] Gonzalez R, Woods R E and Eddins S L 2010 *Digital image processing using MATLAB* 2nd ed (India: McGraw Hill)